

Microstreaming patterns induced by shape modes of acoustically trapped bubbles

Sarah CLEVE⁽¹⁾, Gabriel REGNAULT⁽²⁾, Cyril MAUGER⁽³⁾, Claude INSERRA⁽⁴⁾, Philippe BLANC-BENON⁽⁵⁾

⁽¹⁾Univ Lyon, École Centrale de Lyon, INSA de Lyon, CNRS, LMFA UMR 5509, Écully, France, sarah.cleve@ec-lyon.fr

⁽²⁾Univ Lyon, École Centrale de Lyon, INSA de Lyon, CNRS, LMFA UMR 5509, Écully, France, gabriel.regnault@insa-lyon.fr

⁽³⁾Univ Lyon, INSA de Lyon, École Centrale de Lyon, CNRS, LMFA UMR 5509, Villeurbanne, France,
cyril.mauger@insa-lyon.fr

⁽⁴⁾Univ Lyon, Université Lyon 1, Centre Léon Bérard, INSERM, LabTAU, Lyon, France, claude.inserra@inserm.fr

⁽⁵⁾Univ Lyon, École Centrale de Lyon, INSA de Lyon, CNRS, LMFA UMR 5509, Écully, France,
philippe.blanc-benon@ec-lyon.fr

Abstract

The combination of volumic, translational and nonspherical bubble oscillations induces a relatively slow mean flow, called microstreaming, in the vicinity of the bubble. It is well known that microstreaming and its resulting shear stresses play an important role in medical applications such as sonoporation (permeabilization of a cell membrane). The exact mechanisms occurring between bubbles, fluid and biological matter are however not fully understood. Only few studies have tried to correlate the relatively slow streaming to the fast temporal bubble dynamics. In the present work, we visualize for the first time microstreaming around an acoustically trapped bubble that is oscillating with axisymmetric shape modes. Different types of streaming patterns can be observed. Correlation to the temporal bubble dynamics allows us to identify several important parameters that define the patterns of microstreaming. As might be expected the mode number plays an important role, nevertheless it is not sufficient to define a streaming pattern. Phase differences between several modal components as well as the bubble size with respect to the resonance frequency have to be taken into account as well.

Keywords: Microstreaming, bubble, nonspherical oscillations

1 INTRODUCTION

Micrometer sized bubbles find use in diagnostic and therapeutic medical applications. One of those applications is sonoporation, the permeabilization of a cell membrane. Amongst possible mechanisms that may lead to sonoporation, bubble-induced microstreaming and its related shear stress are supposed to play a key role. This was evidenced by Wu et al. [1] and Marmottant et al. [2] who respectively produce streaming around a Mason horn tip or generated by microbubbles. Investigations of microstreaming commonly refer to bubbles attached to a wall [3] allowing the identification of the different pattern types [4]. However, there are no detailed studies on microstreaming induced by a single bubble far from any boundary. Furthermore, most existing studies on microstreaming do not correlate the streaming to its cause, that means to the bubble dynamics. While extensive microstreaming observations and modelling have been performed for bubbles combining radial oscillations and translational motions, few studies are dedicated to the combination of spherical and surface oscillations, that have been evidenced to lead to large amplitudes of bubble interface motion [5].

In the present study, we aim to characterize microstreaming induced by such a single bubble far from any boundary and to correlate it to the bubble dynamics. We are in particular interested in the effect of surface modes on the streaming pattern.

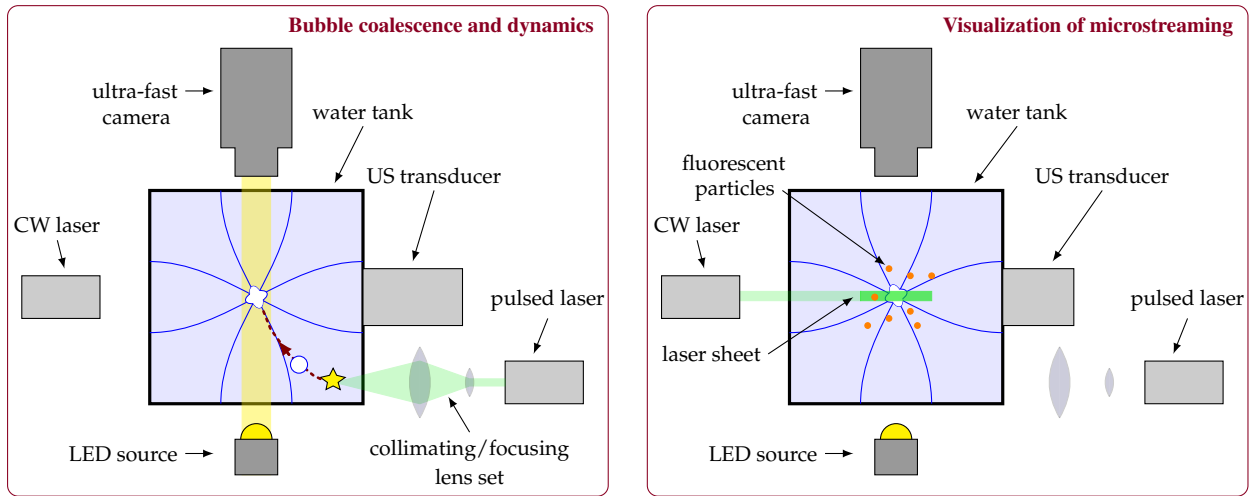


Figure 1. Schematic representation of the experimental setup; *left*: creation of bubbles by short laser pulses, trapping in the acoustic field and triggering of surface modes via bubble coalescence. The camera and light source allow the visualization of the bubble dynamics; *right*: visualization of microstreaming with fluorescent tracer particles and a laser sheet.

2 EXPERIMENTAL SETUP AND PROCEDURE

The experiments consist of two steps. In a first step surface modes are triggered, in a second step bubble dynamics and microstreaming are recorded.

2.1 Experimental setup

The experimental setup, see figure 1, consists of a 8 cm cubic water tank filled with non-degassed water. Single bubbles are nucleated by short laser pulses ($\lambda = 532\text{nm}$, second harmonic of a Nd:YAG pulsed laser, New Wave Solo III, 6ns pulse duration). An ultrasonic plane transducer (SinapTec®, diameter of the active area 35mm) is attached to the bottom of the tank and driven at 31.25kHz. All bubbles are smaller than resonant size and are hence attracted to the pressure antinodes of the standing acoustic field. Experiments are captured with a CMOS camera (Vision Research® V12.1) equipped with a $12\times$ objective lens (Navitar® equipped with an additional $1.5\times$ lense). For the visualization of the bubble dynamics, backlight imaging with a LED light source is used. For the visualization of streaming, a continuous wave laser source ($\lambda = 532\text{nm}$, DPSS, CNI MLL-FN, 400mW) is used and a thin laser sheet is formed. Red fluorescent polymer microspheres (diameter, $0.71\mu\text{m}$, Duke Scientific) are added to the water as flow tracers.

2.2 Triggering of surface modes

In order to obtain surface modes, we use bubble coalescence. The method is explained in detail elsewhere [6], the main idea is the following. Performing controlled experiments on microstreaming lead to two requirements for the surface modes, (1) controlled orientation of the bubble symmetry and (2) steady-state oscillations of the bubble. Both requirements are fulfilled with the method of bubble coalescence. It is worth noting that the mode number can be predicted through the choice of the parameters bubble radius R_0 , acoustic pressure p_a and driving frequency f_{ac} [7].

An example bubble coalescence is shown in figure 2. The approach is followed by film rupture between the bubbles, leading to an initial shape-deformed bubble. Being acoustically driven this bubble will exhibit transient

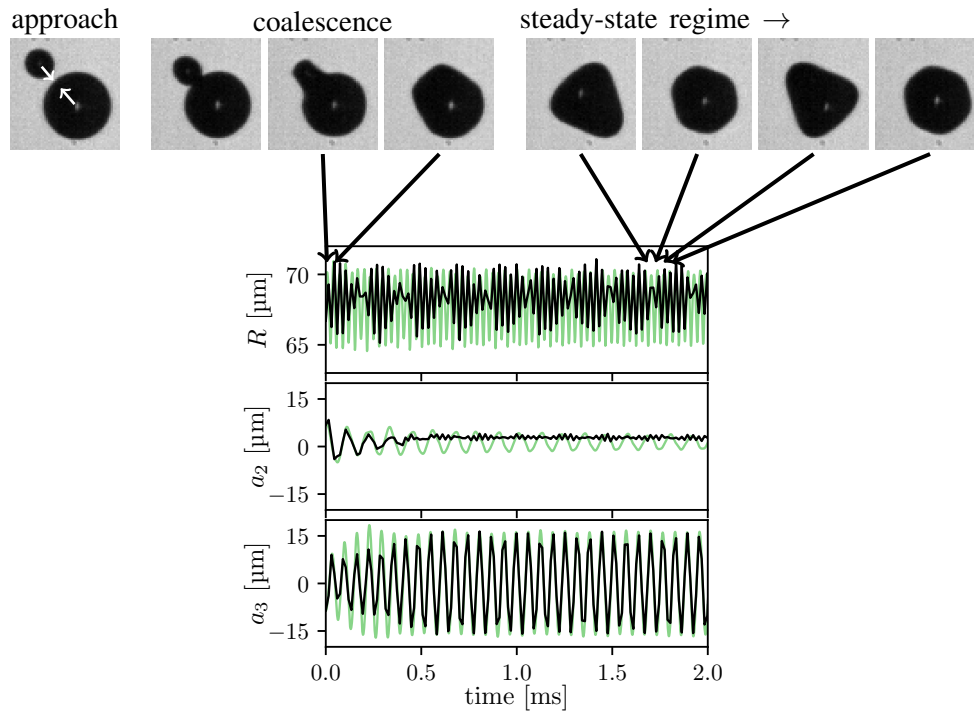


Figure 2. Example snapshot of bubble coalescence (frame size $220 \times 220 \mu\text{m}$). After the approach, the two bubbles coalesce at the time defined as $t = 0 \text{ ms}$. After a relatively short time, the steady-state regime is reached. The plot shows the modal decomposition for the radial mode R and the modes 2 and 3. As can be seen on the snapshots, the modals amplitude a_2 becomes negligible while the maximum modal amplitude a_3 reaches a steady state value. Note that the experimental values (black line) are superposed with a numerical simulation (green line) according to the coupled-mode theory of volumic and nonspherical oscillation [8].

nonspherical oscillations, and after a sufficient number of acoustic cycles a steady-state regime is reached. As a result, we dispose of one bubble oscillating on a surface mode (here mode 3) in the steady-state regime and a controlled axis of symmetry (which equals the axis along which the two bubbles approach each other just before coalescence).

2.3 Visualization of microstreaming and bubble dynamics

Once a surface mode is triggered, quickly alternating recordings of the bubble dynamics, figure 1 left, and microstreaming, figure 1 right, are made. The bubble dynamics is recorded at a frame rate of 180kfps and image analysis is done to extract the information on the bubble dynamics. Microstreaming is a relatively slow phenomenon compared to the fast bubble dynamics. Recordings are done at about 500fps. The videos are analysed by two methods. The first method is the so called streak photography, where all obtained snapshots are superposed and only minimum values for every pixel are kept. The result, see figure 3 on the left, reveals the trajectories of the tracer particles. The second method is particle image velocimetry (PIV). Figure 3 shows the corresponding result to the streak photography on the left.

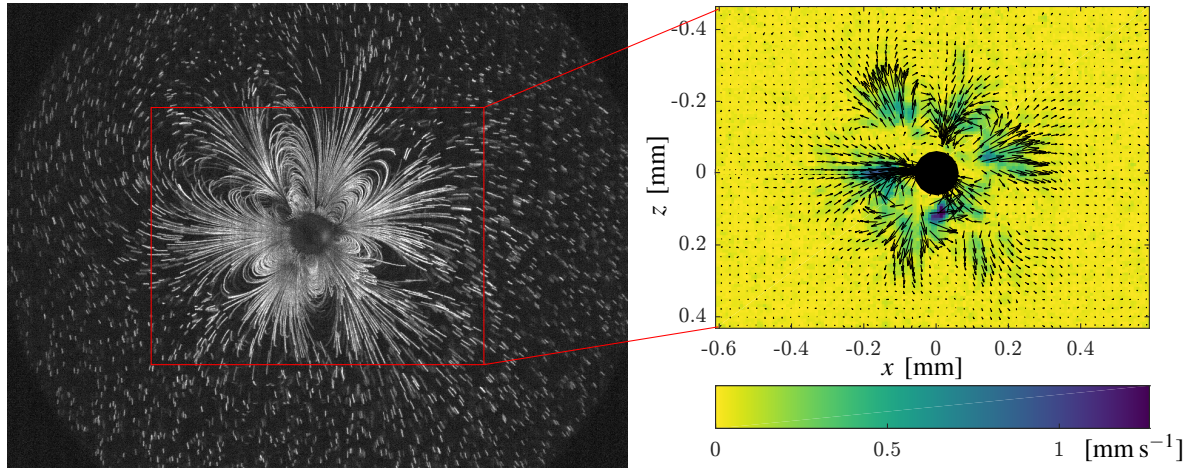


Figure 3. Microstreaming around a bubble oscillating on a mode 3. On the streak image (left), six lobes are visible. The PIV result reveals maximum velocities of the order of 1 mm s^{-1} .

3 RESULTS AND DISCUSSION

In the following is detailed a study on microstreaming induced by an acoustically trapped bubble that is oscillating with surface modes.

Intuitively, the streaming patterns induced by a bubble will depend on the predominant mode n of the bubble oscillations and more specifically one might expect a streaming pattern with $2n$ lobes. However, this assumption is a too large simplification and does not correspond to the complete results. Four example patterns, that underline this statement, are shown in figure 4. It is true that we do observe $2n$ lobes, here 6 lobes for the mode 3 in the upper right example and 8 lobes for the mode 4 in the lower right one. On the left side we see however two examples for a mode 3 and 4 respectively, which lead to larger cross-like patterns.

Through classification of the different examples we found that the bubble size plays an important role in the distinction between the two cases. For the mode 3, the example on the upper left of figure 4 showing a large cross-like pattern corresponds to a bubble with a radius of $\approx 65 \mu\text{m}$, which is smaller than the resonant size of the mode 3 ($\approx 67 \mu\text{m}$). The example on the upper right of figure 4 showing a pattern with six lobes around the bubble corresponds to a bubble with a radius of $\approx 70 \mu\text{m}$, which is larger than the resonant size of the mode 3. The same observation can be made for mode 4 oscillations: smaller bubbles show large cross-like patterns (lower left example of figure 4) and larger bubbles show lobes confined around the bubble (lower right example of figure 4).

Possible reasons for this separation are the following. First of all, the modal content is not the same below and above the resonant size $R_{\text{res},n}$ [9]. Furthermore, the equations of the surface dynamics reveal that different phase lags may occur on either side of $R_{\text{res},n}$.

The control of such streaming patterns might find application in different small-scale applications. For micromixing with acoustically excited bubbles it is helpful to understand the extent of the streaming, a relatively small lobe-shaped pattern and a large cross-like one obviously not leading to the same effects on the surrounding. Further applications can be found in medical field, where streaming may result for instance in the permeabilization of a cell membrane (sonoporation). Controlling the extent of the streaming pattern can help to localize the therapeutic effect.

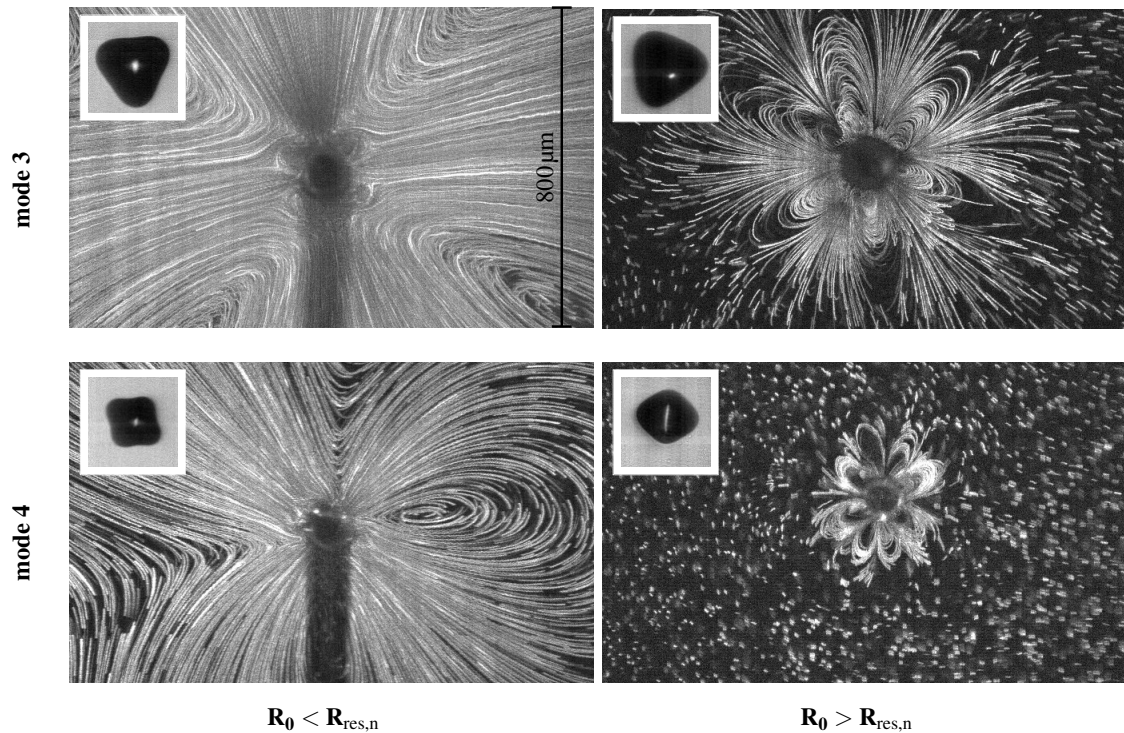


Figure 4. Four examples of microstreaming patterns. The upper row shows two examples for a mode 3, the lower row two examples for a mode 4 (see snapshots of the respective dynamics in the respective inlets). Two types of patterns are observed: the examples on the left are large cross-like patterns for bubbles that are smaller than the respective resonant size ($R_{\text{res},3} \approx 54\mu\text{m}$ and $R_{\text{res},4} \approx 67\mu\text{m}$), the examples on the right are confined lobes patterns for bubbles that are larger than the respective resonant size. The radii are in the upper left case $R_0 \approx 65\mu\text{m}$, in the upper right $R_0 \approx 70\mu\text{m}$, in the lower left $R_0 \approx 53\mu\text{m}$, and in the lower right $R_0 \approx 55\mu\text{m}$.

4 CONCLUSION

In the present work we show microstreaming around an acoustically trapped bubble. A large number of patterns can be observed. A classification into two groups is possible, large mostly cross-like patterns and smaller patterns with confined lobes. For modes 3 and 4 we observed that a distinction is obtained when classing them according to the respective bubble size.

The finding of this work are expected to play a role in small-scale applications such as micromixing and medical applications such as sonoporation.

ACKNOWLEDGEMENTS

This work was performed within the framework of the Labex CeLyA of the Université de Lyon, within the programme 'Investissements d'Avenir' (ANR-10-LABX-0060/ANR-16-IDEX-0005) operated by the French National Research Agency (ANR).

REFERENCES

- [1] Wu, J.; Ross, J. P.; Chiu, J.-F. Reparable sonoporation generated by microstreaming, *The Journal of the Acoustical Society of America*, Vol 111, 2002, pp 1460-1464.
- [2] Marmottant, P.; Hilgenfeldt, S. Controlled vesicle deformation and lysis by single oscillating bubbles, *Nature*, Vol 423, 2003, pp 153-156.
- [3] Marmottant, P.; Raven, J.; Gardeniers, H.; Bomer, J.; Hilgenfeldt, S. Microfluidics with ultrasound-driven bubbles, *Journal of Fluid Mechanics*, Vol 568, 2006, pp 109-118.
- [4] Tho, P.; Manasseh, R.; Ooi, A. Cavitation microstreaming patterns in single and multiple bubble systems, *Journal of Fluid Mechanics*, Vol 576, 2007, pp 191-233.
- [5] Guédra, M.; Cleve, S.; Mauger, C.; Blanc-Benon, P.; Inserra, C. Dynamics of nonspherical microbubble oscillations above instability threshold, *Physical Review E*, Vol 96, 2017, 063104.
- [6] Cleve, S.; Guédra, M.; Mauger, C.; Inserra, C.; Blanc-Benon, P. Surface modes with controlled axisymmetry triggered by bubble coalescence in a high-amplitude acoustic field, *Physical Review E*, Vol 98, 2018, 033115.
- [7] Brenner, M. P.; Lohse, D.; Dupont, T. F. Bubble shape oscillations and the onset of sonoluminescence, *Physical Review Letters*, Vol 75, 1995, 954.
- [8] Shaw, S. J. Translation and oscillation of a bubble under axisymmetric deformation, *Physics of Fluids*, Vol 18, 2006, 072104.
- [9] Guédra, M. and Inserra, C. Bubble shape oscillations of finite amplitude, *Journal of Fluid Mechanics*, Vol 857, 2018, pp 681-703.